EXHIBIT D

differed between NMDA and KA (Fig. 3*c*, *d*), and in individual spinal cord neurones KA-evoked increases in $[Ca^{2+}]_i$ were always much smaller than those evoked by NMDA. These experiments suggest that Na^+ is a poor trigger for inducing an increase in $[Ca^{2+}]_i$, since in several neurones the inward (Na^+) current activated by KA produced no detectable arsenazo III signal. However, our results do not exclude the possibility that Ca^{2+} influx through ion channels activated by NMDA triggers release of Ca^{2+} from intracellular stores[27], contributing further to the NMDA-evoked arsenazo III signals reported here. Although the present results suggest a high Ca^{2+} permeability of NMDA-receptor-activated channels (Fig. 3), the net flux of monovalent cations (that is, conductance) decreases in the presence of Ca^{2+}. This reflects interactions between permeant ions within the channel with Ca^{2+} acting as both a permeant ion and as a blocker of monovalent cation flux[25,26,28].

The experiments reported here provide evidence for an agonist-triggered increase in $[Ca^{2+}]_i$ in mammalian spinal cord neurones. Previously, ion-sensitive microelectrodes were used to measure changes in intracellular ionic activity triggered by excitatory amino acids in frog motoneurones[9]. The latter experiments suggested an increase in both $[Na^+]_i$ and $[Ca^{2+}]_i$ during perfusion with L-glutamate but the results were difficult to interpret clearly as (1) neurones were not voltage-clamped and thus it is difficult to separate the relative contributions of Ca^{2+} influx via voltage-dependent calcium channels and agonist-activated channels, and (2) L-glutamate is a mixed agonist that acts at multiple subtypes of excitatory amino-acid receptor[2,6,7].

The response to NMDA-receptor activation thus provides a second source of calcium flux, distinct from that resulting from conventional voltage-dependent calcium channels, which may have important long-term effects on excitability. Our finding that the ion channels linked to the NMDA receptor subtype are more permeable to Ca^{2+} than those linked to KA receptors, has implications for the role of excitatory amino-acid receptors in CNS function. It is possible that Ca^{2+} influx activated by NMDA receptors underlies the synaptic plasticity generating long-term potentiation, as the latter is prevented by intracellular injection of EGTA to chelate Ca^{2+} (ref. 29), or by blocking NMDA receptors with selective antagonists[30]. For example, Ca^{2+} influx localized at transmitter-operated ion channels could have a role in organizing and regulating postsynaptic structures in an appropriate spatial relation to transmitter-releasing presynaptic terminal boutons, and it is important to consider that Ca^{2+} influx occurring at NMDA receptors located on dendritic spines might produce an especially large but localized elevation in intracellular Ca^{2+} concentration, due to restriction of Ca^{2+} diffusion along the narrow shaft of the spine. In addition, our results have some bearing on the mechanisms of desensitization of NMDA receptors, as the link that has been demonstrated between $[Ca^{2+}]_i$ and desensitization of nicotinic receptors at the neuromuscular junction[31,32] may occur also for other receptor–ionophore complexes. Thus our results may help to explain the similar desensitization evoked by either large doses of NMDA or depolarizing voltage jumps[7], which trigger Ca^{2+} entry through NMDA channels and voltage-dependent calcium channels, respectively.

Received 3 January; accepted 1 April 1986.

1. Krogsgaard-Larsen, P., Honoré, T., Hansen, J. J., Curtis, D. R. & Lodge, D. *Nature* **284**, 64–66 (1980).
2. Watkins, J. C. & Evans, R. H. *A. Rev. Pharmac. Tox.* **21**, 165–205 (1981).
3. McLennan, H. *Prog. Neurobiol.* **20**, 251–271 (1983).
4. Nowak, L., Bregestovski, P., Ascher, P., Herbet, A. & Prochiantz, A. *Nature* **307**, 462–465 (1984).
5. Mayer, M. L., Westbrook, G. L. & Guthrie, P. B. *Nature* **309**, 261–263 (1984).
6. Mayer, M. L. & Westbrook, G. L. *J. Physiol., Lond.* **354**, 29–53 (1984).
7. Mayer, M. L. & Westbrook, G. L. *J. Physiol., Lond.* **361**, 65–90 (1985).
8. Dingledine, R. *J. Physiol., Lond.* **343**, 385–405 (1983).
9. Bührle, C. P. & Sonnhof, U. *Pflügers Arch. ges. Physiol.* **396**, 154–162 (1983).
10. Zanotto, L. & Heinemann, U. *Neurosci. Lett.* **35**, 79–84 (1983).
11. Pumain, R. & Heinemann, U. *J. Neurophysiol.* **53**, 1–16 (1985).
12. Lansman, J. B., Hess, P. & Tsien, R. W. *J. gen. Physiol.* (in the press).
13. Ault, B., Evans, R. H., Francis, A. S., Oakes, D. J. & Watkins, J. C. *J. Physiol., Lond.* **307**, 413–428 (1980).
14. Crunelli, V. & Mayer, M. L. *Brain Res.* **311**, 392–396 (1984).
15. Hamill, O. P., Marty, A., Neher, E., Sakmann, B. & Sigworth, F. *Pflügers Arch. ges. Physiol.* **391**, 85–100 (1981).
16. Cull-Candy, S. G. & Ogden, D. C. *Proc. R. Soc.* B**224**, 367–373 (1985).
17. Hagiwara, S. & Bylerly, L. *A. Rev. Neurosci.* **4**, 69–125 (1981).
18. Smith, S. J., MacDermott, A. B. & Weight, F. F. *Nature* **304**, 350–352 (1983).
19. Gorman, A. L. F. & Thomas, M. V. *J. Physiol., Lond.* **308**, 259–285 (1980).
20. Berridge, M. J. & Irvine, R. F. *Nature* **312**, 315–321 (1984).
21. Sladeczek, F., Pin, J. P., Récasens, M., Bockaert, J. & Weiss, S. *Nature* **317**, 717–719 (1985).
22. Schoffelmeer, A. M. N. & Mulder, A. H. *J. Neurochem.* **40**, 615–621 (1983).
23. Evans, R. H. & Watkins, J. C. *J. Physiol., Lond.* **277**, 57P (1977).
24. Nowak, L. M. & Ascher, P. *Soc. Neurosci. Abstr.* **10**, 23 (1984).
25. Mayer, M. L. & Westbrook, G. L. *Soc. Neurosci. Abstr.* **11**, 785 (1985).
26. Ascher, P. & Nowak, L. *J. Physiol., Lond. Proc.* (in the press).
27. Fabiato, A. & Fabiato, F. *Ann. N.Y. Acad. Sci.* **307**, 491–522 (1978).
28. Nowak, L. M. & Ascher, P. *Soc. Neurosci. Abstr.* **11**, 953 (1985).
29. Lynch, G., Larson, J., Kelso, S., Barrinuevo, G. & Schottler, F. *Nature* **305**, 719–721 (1983).
30. Collingridge, G. L., Kehl, S. J. & McLennan, H. *J. Physiol., Lond.* **334**, 33–46 (1983).
31. Parsons, R. L. in *Calcium in Drug Action* (ed. Weiss, G. B.) 289–314 (Plenum, New York, 1978).
32. Miledi, R. *Proc. R. Soc.* B**209**, 447–452 (1980).
33. Adams, D. J., Dwyer, T. M. & Hille, B. *J. gen. Physiol.* **75**, 493–510 (1980).
34. Edwards, C. *Neuroscience* **7**, 1335–1366 (1982).

Replacing the complementarity-determining regions in a human antibody with those from a mouse

Peter T. Jones, Paul H. Dear, Jefferson Foote, Michael S. Neuberger & Greg Winter

Laboratory of Molecular Biology, Medical Research Council, Hills Road, Cambridge CB2 2QH, UK

The variable domains of an antibody consist of a β-sheet framework with hypervariable regions (or complementarity-determining regions—CDRs) which fashion the antigen-binding site. Here we attempted to determine whether the antigen-binding site could be transplanted from one framework to another by grafting the CDRs. We substituted the CDRs from the heavy-chain variable region of mouse antibody B1–8, which binds the hapten NP-cap (4-hydroxy-3-nitrophenacetyl caproic acid; $K_{NP\text{-}cap} = 1.2\ \mu M$), for the corresponding CDRs of a human myeloma protein. We report that in combination with the B1–8 mouse light chain, the new antibody has acquired the hapten affinity of the B1–8 antibody ($K_{NP\text{-}cap} = 1.9\ \mu M$). Such 'CDR replacement' may offer a means of constructing human monoclonal antibodies from the corresponding mouse monoclonal antibodies.

The three-dimensional structures of several immunoglobulins show that the variable domains consist of two β-sheets pinned together by a disulphide bridge, with their hydrophobic faces packed together[1–3]. The individual β-strands are linked by loops which at one tip of the β-sheet may fashion a binding pocket for small haptens[1,2]. Sequence comparisons among heavy- and light-chain variable domains (V_H and V_L respectively) reveal that each domain has three CDRs flanked by four relatively conserved regions (framework regions—FRs)[4]. As seen in the structure of the human myeloma protein NEWM (Fig. 1), the CDRs include each of the three main loops. Often the CDRs also include the ends of the β-strands, suggesting that side chains at the ends of the β-strands may help to fix the conformation or orientation of the loops. The framework regions form the bulk of the β-sheet, although for example in the V_H domain of NEWM, FR1 includes part of the loop between the two β-sheets and CDR2 not only forms a loop but a complete β-strand (Fig. 1). The structure of the β-sheet framework is similar in different antibodies, as the packing of different side chains is accommodated by slight shifts between the two β-strands[5]. Furthermore, the packing together of V_L and V_H FRs is conserved[6], therefore the orientation of V_L with respect to V_H is fixed. We wondered whether the FRs represent a simple β-sheet scaffold on which new binding sites may be built, and

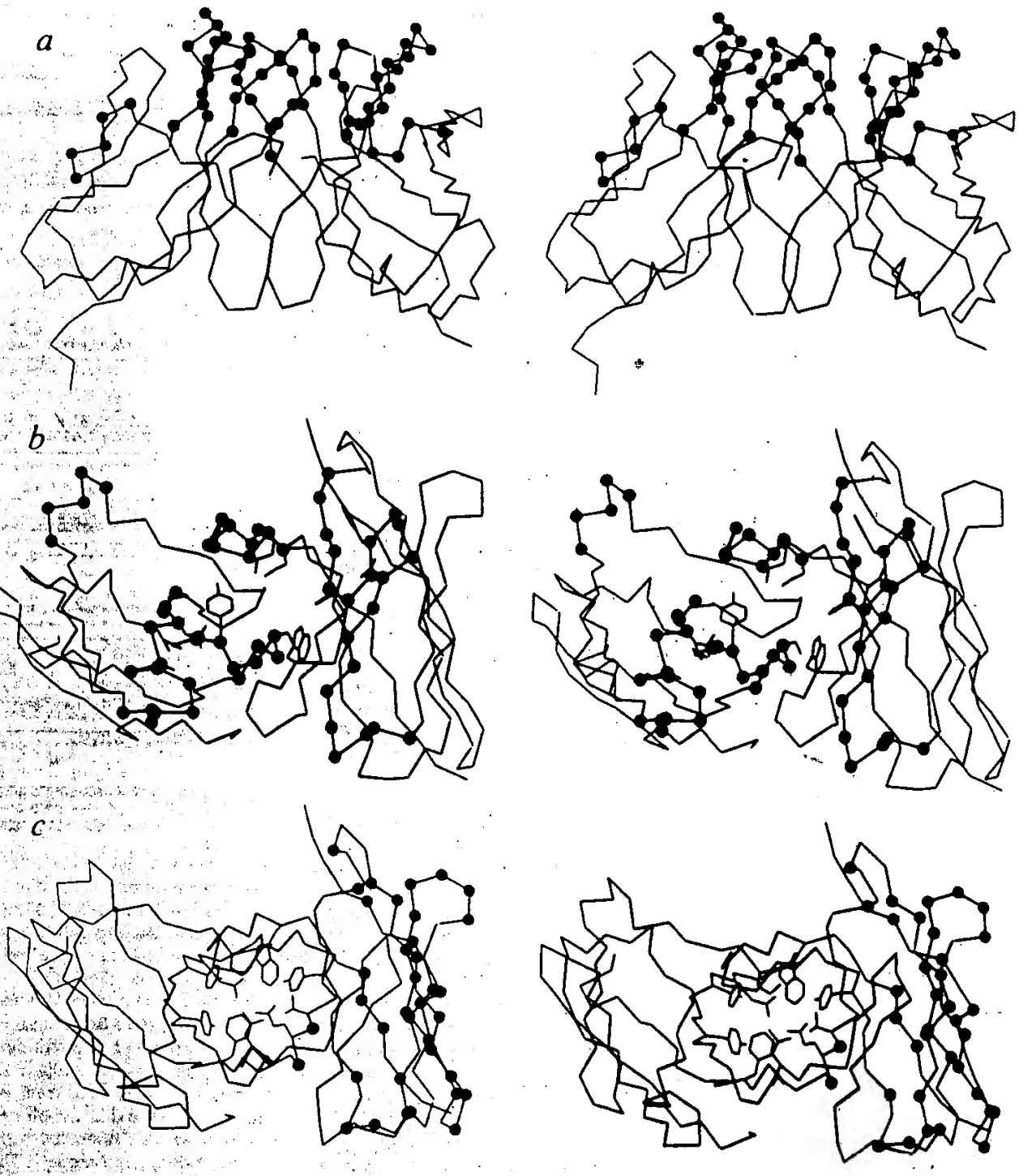

Fig. 1 Stereo pairs of the V_H (right) and V_L (left) domains of the human myeloma protein NEWM[1,8] generated using the computer graphics program FRODO[25]. The tracings indicate the backbone of C^α atoms for the framework regions. *a*, The C^α atoms of the CDRs (●) cluster at the tip of the variable domain. *b*, A view into the hapten binding pocket with the CDRs in the order (clockwise from noon): V_H CDR3, CDR1 and CDR2, and V_L CDR3, CDR1 and CDR2. The side chains lining the binding pocket (V_L A 28, N 30, Y 90, S 93, R 95, V_H W 47, Y 50, F 52, I 100, A 101) lie almost entirely in the CDRs. *c*, The C^α atoms in the NEWM V_H domain are marked (●) where side chains in the mouse B1-8 V_H domain are different. The side chains (V_L Y 35, Q 37, A 42, P 43, Y 86, F 99, V_H V 37, Q 39, L 45, Y 94, W 107) involved in packing V_H and V_L framework regions are traced. In the V_H domain all these side chains are conserved in mouse B1-8.

whether the structure of the CDRs (and antigen binding) is therefore independent of the FR context. To answer these questions experimentally, we have grafted the CDRs from one antibody to another, to determine whether antigen binding transfers with the CDRs.

We grafted the CDRs from the V_H domain of the mouse monoclonal antibody B1-8 (ref. 7) into the V_H domain of the human myeloma protein NEWM, whose crystallographic structure is known[1,8]. The V_H domain of the CDR donor (B1-8) is attached to a μ constant region and associated with a mouse λ1 light chain, and the antibody is directed against the hapten NP-cap. Both the V_H and V_L domains seem to have a role in determining the affinity of the antibody for NP-cap as the substitution of either domain by other, often highly related variable domains can destroy hapten binding (refs 7, 9 and M.S.N., unpublished results). In the V_H domain, each of the CDRs has been implicated in NP-cap binding[10], but the class of constant domains attached to V_H does not seem to affect binding of hapten[11,12]. The CDRs from the V_H domain of antibody B1-8 (ref. 13) are longer than the CDRs which they replace in NEWM[4] and this may give rise to a deeper binding pocket.

Most of the residues conserved between the V_H domains of B1-8 and NEWM are located in FR2, FR4 and the carboxy-terminal third of FR3 (Fig. 2*a*) and largely form the region of β-sheet which is packed against the light chain. Therefore, it might be expected that the V_H domain of B1-8 (hereafter abbreviated to MV_{NP}) and the hybrid B1-8/NEWM domain (HuV_{NP}) would dock in a similar manner with the mouse V_L domain to form the antigen-combining site[6]. The more variable FR1 and N-terminal two-thirds of FR3 form the other β-sheet which is exposed to solvent (Fig. 1*c*).

The gene encoding the HuV_{NP} domain was constructed by gene synthesis (Fig. 2*b*). We then constructed a plasmid, pSV-$HuV_{NP}H\varepsilon$, in which the HuV_{NP} domain is linked to a human ε constant region, and cloned into a pSV2gpt-derived vector[14]. The plasmid DNA was introduced into cells of the J558L mouse myeloma by spheroplast fusion. J558L secretes λ1 light chains which have been shown to associate with heavy chains containing a MV_{NP} variable domain, to create a binding site for NP-cap or the related hapten NIP-cap (3-iodo-4-hydroxy-5-nitrophenylacetyl caproic acid)[7]. As the plasmid pSV-$HuV_{NP}H\varepsilon$ contains the *gpt* marker (encoding guanine phosphoribosyltransferase), stably transfected myeloma cells could be selected in medium containing mycophenolic acid[14]; transfectants would be expected to secrete an antibody (HuV_{NP}-IgE) with a heavy chain composed of a HuV_{NP} variable domain and human ε constant regions, and the λ1 light chain of the J558L myeloma. The culture supernatants of several gpt^+ clones were assayed by radioimmunoassay and found to contain NIP-cap-binding antibody. The antibody secreted by one such clone was purified from the culture supernatant by affinity chromatography on NIP-cap–Sepharose, and by SDS-polyacrylamide gel electrophoresis the protein was indistinguishable from the mouse chimaeric MV_{NP}-IgE (ref. 12) (results not shown). The HuV_{NP}-IgE antibody competes effectively with MV_{NP}-IgE for binding to both anti-human ε (Fig. 3*a*) and NIP-cap coupled to bovine serum albumin (NIP-BSA) (Fig. 3*b*).

The affinities of HuV_{NP}-IgE for NP-cap and NIP-cap were

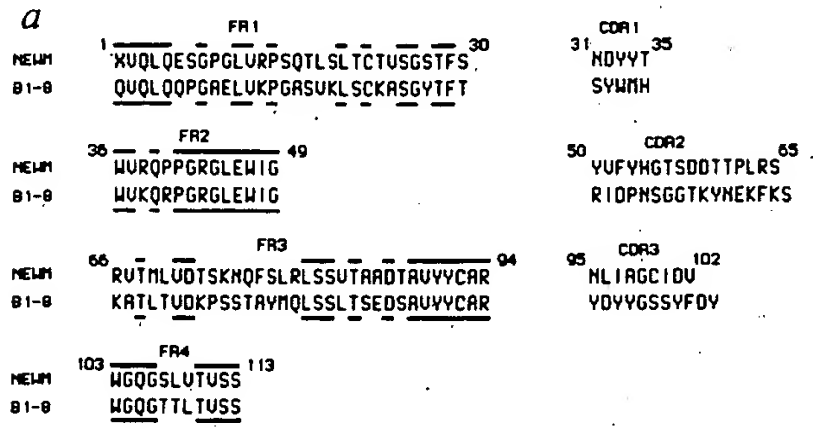

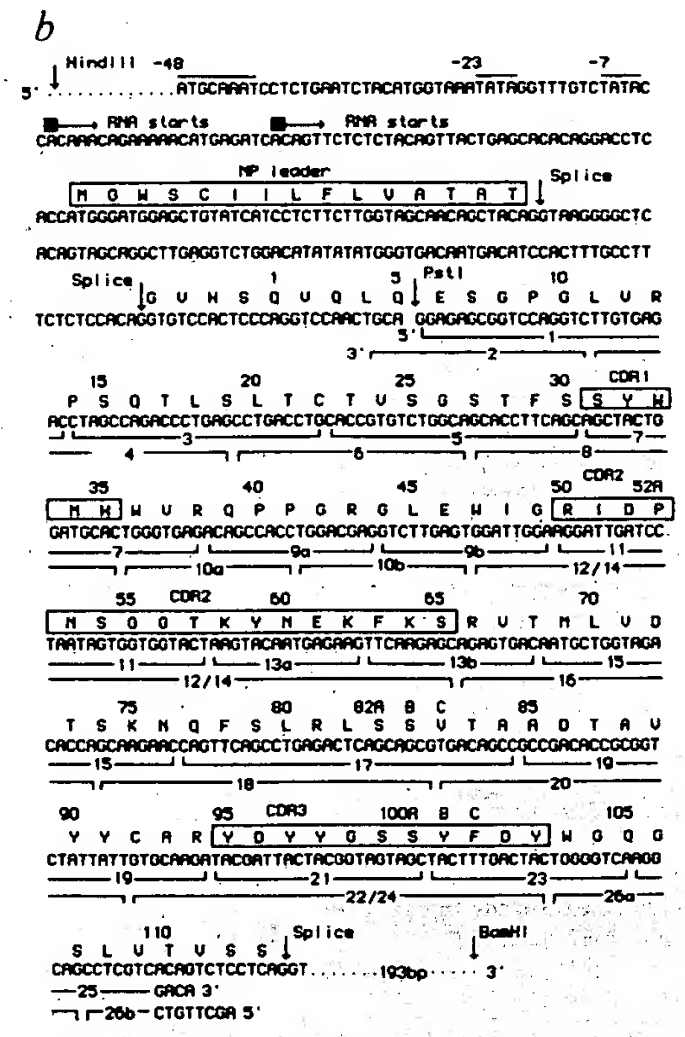

Fig. 2 *a*, Amino-acid sequence of the V_H domain of the human myeloma protein NEWM compared with that of the mouse B1-8 (anti-NP) antibody, and divided into FRs and CDRs according to Kabat *et al.*[4]. Conserved residues are marked with a line above and below the residue. *b*, Amino-acid and nucleotide sequence of the HuV_{NP} gene, in which the CDRs from the V_H domain of the mouse B1-8 antibody alternate with the FRs of human NEWM protein. The gene was constructed by replacing a section of the MV_{NP} gene in the vector pSV-V_{NP} (ref. 12) with a synthetic fragment encoding the HuV_{NP} domain. Thus the 5′ and 3′ noncoding sequences, the leader sequence, the leader-variable region intron, five N-terminal and four C-terminal amino acids are derived from the MV_{NP} gene; the rest of the coding sequence is derived from the synthetic HuV_{NP} fragment. The oligonucleotides are aligned with the corresponding portions of the HuV_{NP} gene. For convenience in cloning, the ends of oligonucleotides 25 and 26b form a *Hin*dII site followed by a *Hin*dIII site, and the sequences of the 25/26b oligonucleotides therefore differ from the HuV_{NP} gene.

Methods. The synthetic gene for HuV_{NP} was constructed as a *Pst*I-*Hin*dIII fragment. The nucleotide sequence was derived from the protein sequence using the computer program ANALYSEQ[26] with optimal codon usage taken from the sequences of mouse constant-region genes. The oligonucleotides used in synthesis (1-26b, 28 in total) vary in size from 14 to 59 bases and were made on a Biosearch SAM or an Applied Biosystems machine, and purified on 8 M urea/polyacrylamide gels[27]. The oligonucleotides were assembled in eight single-stranded blocks (A-D and A′-D′) containing oligonucleotides 1, 3, 5 and 7 (block A), 2, 4, 6 and 8 (block A′), 9, 11, 13a and 13b (block B), 10a, 10b and 12/14 (block B′), 15 and 17 (block C), 16 and 18 (block C′), 19, 21, 23 and 25 (block D), and 20, 22/24, 26a and 26b (block D′). In a typical assembly, for example of block A, 50 pmol of oligonucleotides 1, 3, 5 and 7 were phosphorylated at the 5′ end with T_4 polynucleotide kinase and mixed with 5 pmol of the terminal oligonucleotide which had been phosphorylated with 5 μCi of [γ-^{32}P]ATP (Amersham; 3,000 Ci mmol^{-1}). These oligonucleotides were annealed by heating to 80 °C and cooling to room temperature over 30 min with unkinased oligonucleotides 2, 4 and 6 as splints in 150 μl of 50 mM Tris-HCl *p*H 7.5, 10 mM $MgCl_2$. For the ligation, ATP (1 mM) and dithiothreitol (10 mM) were added, together with 50 units of T_4 DNA ligase (Anglian Biotechnology Ltd), and the mixture was incubated for 30 min at room temperature. EDTA was added to 10 mM, the sample extracted with phenol, precipitated from ethanol, dissolved in 20 μl of water and boiled for 1 min with an equal volume of formamide dyes. Then the sample was loaded onto a thin (0.3 mm) 8 M urea/10% polyacrylamide gel[27] and a band of the expected size detected by autoradiography and eluted by soaking. The two full-length single strands were assembled from A-D and A′-D′ using splint oligonucleotides; thus, A-D were annealed and ligated in 30 μl as above with 100 pmol each of oligonucleotides 10a, 16 and 20 as splints, then incubated overnight (A′-D′ were constructed with oligonucleotides 7, 13b and 17 as splints). After phenol/ether extraction blocks A-D were annealed with blocks A′-D′, small amounts were cloned in the vector M13 mp18 (ref. 28) then cut with *Pst*I and *Hin*dIII, and the gene sequenced by the dideoxy technique[29]. The MV_{NP} gene was transferred as a *Hin*dIII-*Bam*HI fragment from the vector pSV-V_{NP} (ref. 12) to the vector M13mp8 (ref. 30). To facilitate the replacement of MV_{NP} coding sequences by the synthetic HuV_{NP} fragment, three *Hin*dII sites were removed from the 5′ noncoding sequence by site-directed mutagenesis, and a new *Hin*dII site subsequently introduced near the end of FR4. By cutting the vector with *Pst*I and *Hin*dII, most of the V_{NP} coding sequence falls out and the synthetic fragment could be introduced as a *Pst*I-*Hin*dII fragment. The sequence at the *Hin*dII site was corrected to give NEWM FR4 by site-directed mutagenesis. The *Hin*dIII-*Bam*HI fragment, now carrying the HuV_{NP} gene, was excised from M13 and cloned back into pSV-V_{NP} to replace the MV_{NP} gene (and yield the vector pSV-HuV_{NP}). Finally, the heavy-chain constant domains of human IgE (ref. 31) were introduced as a *Bam*HI fragment to yield the vector pSV-$HuV_{NP}H_\varepsilon$, which was transfected into the myeloma line J558L by spheroplast fusion. The sequence of the HuV_{NP} gene in pSV-$HuV_{NP}H\varepsilon$ was checked by re-cloning the *Hin*dIII-*Bam*HI fragment back into M13mp8 (ref. 30).

Table 1 Affinity of HuV_{NP}-IgE and MV_{NP}-IgE for the haptens NP-cap and NIP-cap

	$K_{NP\text{-}cap}$ (μM)	$K_{NIP\text{-}cap}$ (μM)
MV_{NP}-IgE	1.2 ± 0.1	0.02 ± 0.01
HuV_{NP}-IgE	1.9 ± 0.2	0.07 ± 0.02

The affinity of HuV_{NP}-IgE and MV_{NP}-IgE for NP-cap was determined by fluorescence quenching with excitation at 295 nm and emission observed at 340 nm (ref. 22). Antibody solutions were diluted to 100 nM in phosphate-buffered saline, filtered (0.45 μm-pore cellulose acetate) and titrated with NP-cap in the range 0.2-20 μM. As a control, the mouse D1-3 antibody[23], which does not bind hapten, was titrated in parallel. A decrease in the ratio of the fluorescence of HuV_{NP}-IgE or MV_{NP}-IgE (as appropriate) to that of the D1-3 antibody was taken as being proportional to NP-cap occupancy of the antigen-binding sites. The maximum quench was ~40% for both HuV_{NP}-IgE and MV_{NP}-IgE, and hapten dissociation constants were determined from least-squares fits of triplicate data sets to a hyperbola. The concentration of NIP-cap was varied from 10 to 300 nM, and ~50% quenching of fluorescence was observed at saturation. As the antibody concentrations were comparable to the values of the dissociation constants, data were fitted by least-squares to an equation[24] describing tight binding inhibition.

then measured directly using the fluorescence quench technique, and compared with those of MV_{NP}-IgE (Table 1). The antibodies HuV_{NP}-IgE and MV_{NP}-IgE have similar affinities for either hapten (NP-cap or NIP-cap), and although the affinity of HuV_{NP}-IgE for both haptens is slightly lower than that of MV_{NP}-IgE (2-3-fold, 0.3-0.6 kcal mol^{-1}), the difference in affinity is less than expected for loss of either a hydrogen bond or van der Waals' contact from the active site of an enzyme[15,16]. Thus, it seems that binding affinity and specificity for hapten can be conferred on a human antibody by grafting in the CDRs from an appropriate mouse antibody.

Is this result likely to be general? This would assume (1) that antigen usually binds to the CDRs, and any contacts to the FRs are made to the polypeptide backbone or to conserved side chains, and (2) that substitutions in the FRs do not usually affect the conformation of the CDR loops. These assumptions seem reasonable: thus, in the structure of a complex of the D1-3 antibody with lysozyme (R. A. Mariuzza, S. Phillips and R. J. Poljak, personal communication) most contacts to the lysozyme are made by the CDRs, but there is also a hydrogen bond in FR1 of the V_H domain from the β-OH of Thr 30 (often conserved or replaced by Ser). Similarly, the conformation of CDR loops

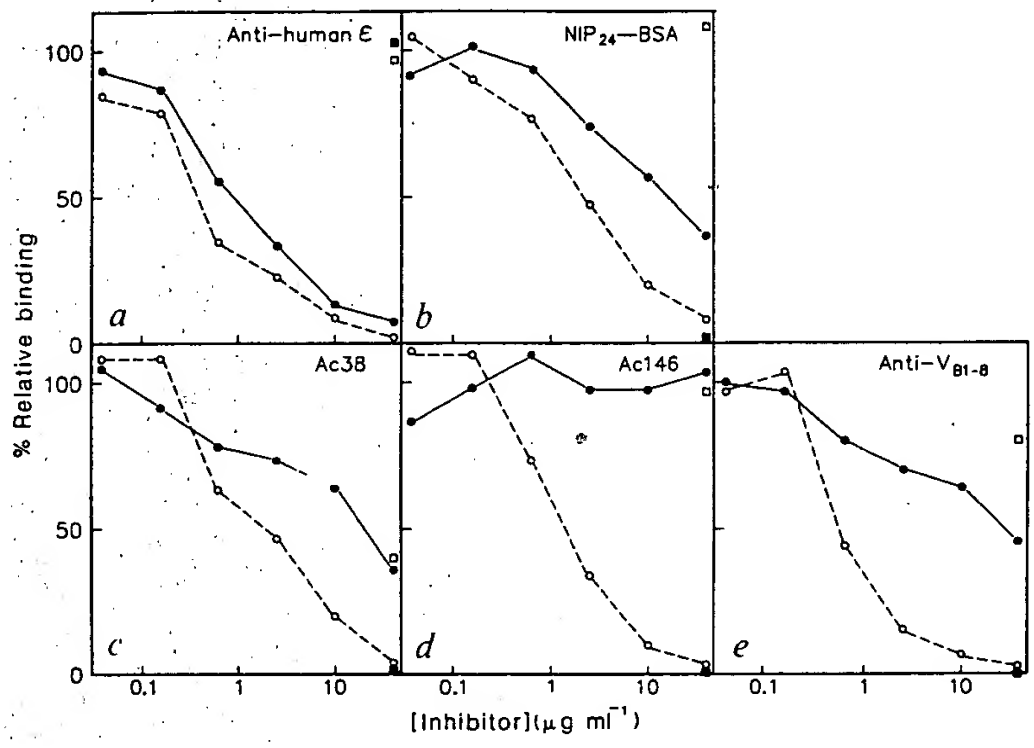

Fig. 3 Comparison of HuV_{NP} and MV_{NP} IgEs in binding inhibition assays. Various concentrations of HuV_{NP}-IgE (●) and MV_{NP}-IgE (○) were used to compete the binding of radiolabelled MV_{NP}-IgE to polyvinyl microtitre plates that had been coated with *a*, sheep anti-human ε antiserum (Seward Laboratory); *b*, $(NIP\text{-}cap)_{24}$–BSA; *c*, Ac38 anti-idiotypic antibody; *d*, Ac146 anti-idiotypic antibody; *e*, rabbit anti-MV_{NP} antiserum. Binding was also carried out in the presence of MV_{NP}-IgM antibody JW1/2/2 (ref. 32) (■) as well as in the presence of JW5/1/2 (□), which is an IgM antibody that differs from JW1/2/2 at 13 residues mainly located in V_H CDR2 (M.S.N., unpublished results). Values of binding are relative to the binding in the absence of inhibitor.

between β-strands depends on loop size and specific interactions of the loop back to the β-sheet. However, in the same class of variable domains (V_H, V_κ or V_λ) these interactions are usually conserved (ref. 5 and A. M. Lesk and C. Chothia, personal communication).

While human monoclonal antibodies have therapeutic potential in human disease, they can be difficult to prepare[17] and treatment of patients with mouse monoclonal antibodies often increases the titre of circulating antibody against the mouse immunoglobulin[18]. As chimaeric antibodies containing human constant domains[12,19,20] and variable domains made by grafting mouse CDRs into human FRs, could have therapeutic potential, we wondered whether the HuV_{NP}-IgE antibody loses antigenic determinants associated with the MV_{NP} variable region (idiotopes). The binding of HuV_{NP}-IgE and MV_{NP}-IgE to both monoclonal and polyclonal anti-idiotypic antibodies directed against the MV_{NP} domain was examined by using inhibition assays. As shown in Fig. 3*d*, the HuV_{NP}-IgE antibody has lost the MV_{NP} idiotypic determinant recognized by antibody Ac146 (ref. 21). Furthermore, HuV_{NP}-IgE also binds the antibody Ac38 (ref. 21) less well (Fig. 3*c*), therefore it is not surprising that HuV_{NP}-IgE has lost many of the determinants recognized by a polyclonal rabbit anti-idiotypic antiserum (Fig. 3*e*). While the loss of idiotypic determinants that accompanies 'humanizing' of the V_H region is reassuring in view of potential therapeutic applications, it does suggest that the recognition of the hapten and of anti-idiotypic antibodies is not equivalent. Thus the HuV_{NP}-IgE antibody retains hapten binding but has lost idiotypic determinants, indicating that the immunoglobulin uses different sites to bind hapten and anti-idiotypic antibodies. It appears, therefore, that both FR and CDR side chains form the binding site for these anti-idiotopes, but mainly CDR side chains interact with hapten.

We thank C. Milstein for suggesting this project, K. Rajewsky and M. Reth for the anti-idiotypic antibodies Ac38 and Ac146, and A. M. Lesk, C. Chothia, R. J. Leatherbarrow and C. Milstein for helpful discussions. J.F. is a Fellow of the Jane Coffin Childs Memorial Fund for Medical Research.

Received 17 February; accepted 17 March 1986.

1. Poljak, R. J. *et al. Proc. natn. Acad. Sci. U.S.A.* **70**, 3305–3310 (1973).
2. Segal, D. M. *et al. Proc. natn. Acad. Sci. U.S.A.* **71**, 4298–4302 (1974).
3. Marquart, M., Deisenhofer, J., Huber, R. & Palm, W. *J. molec. Biol.* **141**, 369–391 (1980).
4. Kabat, E. A., Wu, T. T., Bilofsky, H., Reid-Miller, M. & Perry, H. in *Sequences of Proteins of Immunological Interest* (U.S. Department of Health and Human Services, 1983).
5. Lesk, A. M. & Chothia, C. *J. molec. Biol.* **160**, 325–342 (1982).
6. Chothia, C., Novotny, J., Bruccoleri, R. & Karplus, M. *J. molec. Biol.* **186**, 651–663 (1985).
7. Reth, M., Hämmerling, G. J. & Rajewsky, K. *Eur. J. Immun.* **8**, 393–400 (1978).
8. Saul, F. A., Amzel, M. & Poljak, R. J. *J. biol. Chem.* **253**, 585–597 (1978).
9. Brüggemann, M., Radbruch, A. & Rajewsky, K. *EMBO J.* **1**, 629–634 (1982).
10. Reth, M., Bothwell, A. L. M. & Rajewsky, K. in *Immunoglobulin Idiotypes and Their Expression* (eds Janeway, C., Wigzell, H. & Fox, C. F.) 169–178 (Academic, New York, 1981).
11. Neuberger, M. S. & Rajewsky, K. *Proc. natn. Acad. Sci. U.S.A.* **78**, 1138–1142 (1981).
12. Neuberger, M. S. *et al. Nature* **314**, 268–270 (1985).
13. Bothwell, A. L. M. *et al. Cell* **24**, 625–637 (1981).
14. Mulligan, R. C. & Berg, P. *Proc. natn. Acad. Sci. U.S.A.* **78**, 2072–2076 (1983).
15. Fersht, A. R. *et al. Nature* **314**, 235–238 (1985).
16. Fersht, A. R., Wilkinson, A. J., Carter, P. & Winter, G. *Biochemistry* **24**, 5858–5861 (1985).
17. Boyd, J. E., James, K. & McClelland, D. B. L. *Trends Biotechnol.* **2**, 70–77 (1984).
18. Shawler, D. L., Bartholomew, R. M., Smith, L. M. & Dilman, R. O. *J. Immun.* **135**, 1530–1535 (1985).
19. Morrison, S. L., Johnson, M. J., Herzenberg, L. A. & Oi, V. T. *Proc. natn. Acad. Sci. U.S.A.* **81**, 6851–6855 (1984).
20. Boulianne, G. L., Hozumi, N. & Shulman, M. J. *Nature* **312**, 643–646 (1984).
21. Reth, M., Imanishi-Kari, T. & Rajewsky, K. *Eur. J. Immun.* **9**, 1004–1013 (1979).
22. Eisen, H. N. *Meth. med. Res.* **10**, 115–121 (1964).
23. Mariuzza, R. A. *et al. J. molec. Biol.* **170**, 1055–1058 (1983).
24. Segal, I. H. in *Enzyme Kinetics*, 73–74 (Wiley, New York, 1975).
25. Jones, T. A. in *Computational Crystallography* (ed. Sayre, D.) 303–310 (Clarendon, Oxford, 1982).
26. Staden, R. *Nucleic Acids Res.* **12**, 521–538 (1984).
27. Sanger, F. & Coulson, A. *FEBS Lett.* **87**, 107–110 (1978).
28. Yanisch-Perron, C., Vieira, J. & Messing, J. *Gene* **33**, 103–119 (1985).
29. Sanger, F., Nicklen, S. & Coulson, A. R. *Proc. natn. Acad. Sci. U.S.A.* **74**, 5463–5467 (1977).
30. Messing, J. & Vieira, J. *Gene* **19**, 269–276 (1982).
31. Flanagan, J. G. & Rabbitts, T. H. *EMBO J.* **1**, 655–660 (1982).
32. Neuberger, M. S., Williams, G. T. & Fox, R. O. *Nature* **312**, 604–608 (1984).

Regulation of human insulin gene expression in transgenic mice

Richard F Selden*, Marek J. Skośkiewicz†, Kathleen Burke Howie*, Paul S. Russell† & Howard M. Goodman*

Departments of *Molecular Biology and †Surgery, Massachusetts General Hospital, and Departments of *Genetics and †Surgery, Harvard Medical School, Massachusetts General Hospital, Boston, Massachusetts 02114, USA

Insulin is a polypeptide hormone of major physiological importance in the regulation of fuel homeostasis in animals (reviewed in refs 1, 2). It is synthesized by the β-cells of pancreatic islets, and circulating insulin levels are regulated by several small molecules, notably glucose, amino acids, fatty acids and certain pharmacological agents. Insulin consists of two polypeptide chains (A and B, linked by disulphide bonds) that are derived from the proteolytic cleavage of proinsulin, generating equimolar amounts of the mature insulin and a connecting peptide (C-peptide). Humans, like most vertebrates, contain one proinsulin gene[3,4], although several species, including mice[5] and rats[6,7], have two highly homologous insulin genes. We have studied the regulation of serum insulin